Published OnlineFirst August 15, 2017; DOI: 10.1158/2326-6066.CIR-17-0082

Research Article

Cancer Immunology Research

Primary Tumors Limit Metastasis Formation through Induction of IL15-Mediated Cross-Talk between Patrolling Monocytes and NK Cells

Hiroshi Kubo[1,2], Sofia Mensurado[1], Natacha Gonçalves-Sousa[1], Karine Serre[1], and Bruno Silva-Santos[1,3]

Abstract

Metastases are responsible for the vast majority of cancer-related deaths. Although tumor cells can become invasive early during cancer progression, metastases formation typically occurs as a late event. How the immune response to primary tumors may dictate this outcome remains poorly understood, which hampers our capacity to manipulate it therapeutically. Here, we used a two-step experimental model, based on the highly aggressive B16F10 melanoma, that temporally segregates the establishment of primary tumors (subcutaneously) and the formation of lung metastases (from intravenous injection). This allowed us to identify a protective innate immune response induced by primary tumors that inhibits experimental metastasis. We found that in the presence of primary tumors, increased numbers of natural killer (NK) cells with enhanced IFNγ, granzyme B, and perforin production were recruited to the lung upon metastasis induction. These changes were mirrored by a local accumulation of patrolling monocytes and macrophages with high expression of MHC class II and NOS2. Critically, the protective effect on metastasis was lost upon patrolling monocyte or NK cell depletion, IL15 neutralization, or IFNγ ablation. The combined analysis of these approaches allowed us to establish a hierarchy in which patrolling monocytes, making IL15 in response to primary tumors, activate NK cells and IFNγ production that then inhibit lung metastasis formation. This work identifies an innate cell network and the molecular determinants responsible for "metastasis immunosurveillance," providing support for using the key molecular mediator, IL15, to improve immunotherapeutic outcomes. *Cancer Immunol Res; 5(9); 1–9. ©2017 AACR.*

Introduction

Metastases cause more than 90% of deaths linked to solid tumors, and the lung is one of the most common metastatic sites for various tumor types, including melanoma, breast, liver, and stomach cancers. Metastasis is a complex process where cells detach from the primary tumor, cross the extracellular matrix and intravasate, enter the blood circulation, extravasate at distant sites, and colonize niches to start new processes of expansion. In order to thrive, tumor cells must escape immune surveillance pathways mediated by both innate and adaptive cells, especially natural killer (NK) and T cells. The importance of these pathways is exemplified by escape mechanisms targeting antigen presentation—proteasome subunits, TAP1/2, or MHC class I (1)—or NK cell recognition via downregulation of the NKG2D ligands MICA and MICB (2). In addition to NK cells and T cells, myeloid cell polarization can also contribute to immune escape (3, 4). Classically activated macrophages (M1) and neutrophils (N1) are known to carry out antitumor functions, whereas alternatively activated macrophages (M2) and neutrophils (N2) display protumor activities (5, 6). Monocytes can also be segregated into two subtypes consisting of inflammatory classical ($CCR2^{high}$ $Ly6C^{+}$) monocytes and patrolling nonclassical ($CX3CR1^{+}$ $Ly6C^{-}$) monocytes (7). In breast cancer models, classical monocytes are recruited to metastatic sites and promote extravasation and subsequent growth of cancer cells (8). In contrast, it was reported that patrolling monocytes prevent melanoma metastasis to the lung by recruiting NK cells (9).

The prevailing view is that metastasis occurs as a late event in cancer progression (10). However, a few studies have found tumor cells already disseminated from undetectable primary tumors (11, 12). Considering this possibility, it is likely that the immune system, primed by the primary tumor, may operate to prevent metastatic tumor cells to establish in distant locations. Thus, we hypothesized that primary tumors trigger "metastasis immunosurveillance." To test this hypothesis, we developed a two-step model where primary B16F10 melanoma was established subcutaneously and experimental lung metastasis was then induced by intravenous injection. We showed that B16F10 lung metastasis was inhibited in primary tumor-bearing mice compared with primary tumor-free mice. By using depleting antibodies and genetic ablation, we found that NK cells and IFNγ play a critical role in suppressing metastasis establishment in the presence of primary tumors. NK cell activation and IFNγ production were abolished upon IL15 neutralization, which also abrogated

[1]Instituto de Medicina Molecular, Faculdade de Medicina, Universidade de Lisboa, Lisboa, Portugal. [2]Immunology Research Unit, Department of Medical Innovations, Otsuka Pharmaceutical Co., Ltd., Tokushima, Japan. [3]Instituto Gulbenkian de Ciência, Oeiras, Portugal.

Note: Supplementary data for this article are available at Cancer Immunology Research Online (http://cancerimmunolres.aacrjournals.org/).

Corresponding Author: Bruno Silva-Santos, Instituto de Medicina Molecular, Avenida Prof. Egas Moniz, 1649-028 Lisboa, Portugal. Phone: 351-914-538-335; Fax: 351-217-985-142; E-mail: bssantos@fm.ul.pt

doi: 10.1158/2326-6066.CIR-17-0082

Published OnlineFirst August 15, 2017; DOI: 10.1158/2326-6066.CIR-17-0082

the inhibition of metastasis formation by the primary tumor. We identified patrolling monocytes as the critical source of IL15 upstream of NK cell activation and metastasis inhibition. In summary, our work identifies an IL15-dependent patrolling monocyte/NK cell cross-talk that is induced by primary tumors and strongly inhibits experimental metastasis formation in the lung.

Materials and Methods

Mice and tumor cell line

C57BL/6J (B6) wild-type mice were purchased from Charles River Laboratories. B6.IFNγ$^{-/-}$ mice were purchased from The Jackson Laboratory. All animals were females, 7–13 weeks of age, which were aged matched within 3 weeks. Mice were maintained in specific pathogen-free facilities of Instituto de Medicina Molecular (iMM). All experimental procedures were performed in compliance with the relevant laws and institutional guidelines and have been approved by the local ethics committees. The B16F10 and B16F0 melanoma cell lines were purchased and authenticated from ATCC (Manassas); cultured for 1 week; and passaged 8 and 10 times, respectively, before use. Cells were maintained in Dulbecco's modified Eagles' medium (DMEM) with 10% (vol/vol) FCS (Gibco; Life Technologies) and 1% (vol/vol) penicillin/streptomycin (Sigma).

In vivo tumor transplantation

Tumor cells (5×10^4) were injected s.c. in a volume of 50 μL. Tumor volume was measured by using a caliper and calculated as 1/2 (length × width × width). For the resection experiment, primary tumors (1–2 mm largest diameter) were resected on day 7 or 14 after s.c. injection under general anesthesia. For inducing experimental lung metastasis, 1×10^5 tumor cells were injected i.v. via tail vein in a volume of 100 μL. Mice were sacrificed on day 14 after injection, and tissues were isolated and fixed in 4% paraformaldehyde. Lung metastatic nodules present on the surface of the 5 lobes of the lungs per mouse were counted. One picture of the 5 lobes of the lungs per mouse was used to measure the size of lung metastatic foci by NIH ImageJ. Alternatively, where indicated, the secondary transplanted tumor consisted of 1×10^5 luciferase-expressing B16F0 cells injected intraperitoneally. To monitor tumor growth, mice were injected i.p. with 3 mg D-luciferin (PerkinElmer) in PBS and anesthetized 4 min after with 75 mg/kg body weight of ketamine and 1 mg/kgBW of medetomidine. Images were acquired 10 minutes after D-luciferin injection, using a charge-coupled device camera (IVIS, Xenogen, Cliper, LifeSciences), with a 12.5 cm × 12.5 cm field of view, factor 16 of resolution, with a lens aperture of f/1 and an imaging time of 5 minutes. Anesthesia was reversed by i.p. injection of 1 mg/kgBW of Atipamezole. Data were analyzed in the Living Image 3.0 software (Xenogen) and presented as total flux (photons/s). Mice were sacrificed on day 14 post-secondary tumor inoculation and i.p. tumors were weighed.

Cell lineage depletion

For *in vivo* depletion of specific cell lineages, 200 μg of anti-NK1.1 (Bio X Cell, clone PK136), 500 μg anti-CD115 (anti-CSF1R; Bio X Cell, clone AFS98), 500 μg anti-Ly6G (Bio X Cell, clone 1A8) or PBS control was injected i.p. on days −4, −1, and +2 relative to metastasis induction. For *in vivo* depletion of phagocytic cells, 1 mg of clodronate-loaded liposomes (ClodronateLiposomes.org) or PBS liposomes was injected via retro-orbital vein on days −4, −1, and +2 relative to metastasis induction. IL15 neutralization was performed by injecting 8 μg of anti-IL15/IL15R complex (eBioscience, clone GRW15PLZ) i.p. every day from day −1 to day +3 relative to metastasis induction.

Flow cytometry

Pulmonary lymphoid and myeloid cells were obtained from well-perfused whole lung. Lung tissue was finely chopped, digested with Type I collagenase (1 mg/mL; Wortington) and DNase I (50 μg/mL; Sigma) for 45 minutes at 37°C, and filtered through a 70-μm nylon mesh. Lymphoid and myeloid cells were enriched by Percoll density centrifugation and collected from the interface between the 40% and 70% Percoll layers. Blood was collected and put into microtubes containing heparin. Erythrocytes were osmotically lysed using RBC Lysis Buffer (Biolegend). For surface staining, cells were Fc-blocked for 15 minutes with anti-CD16/32 (eBioscience, clone 93) and incubated for 30 minutes with antibodies in PBS with RPMI-1640 medium (Gibco; Life Technologies) supplemented with 10% (vol/vol) FCS, 1% (vol/vol) penicillin/streptomycin, 1% (vol/vol) nonessential amino acids, 10 mmol/L HEPES, 50 μmol/L 2-mercaptoethanol, and 1% (vol/vol) pyruvate and gentamycin (10 μg/mL). Monoclonal antibodies (mAb) for the following markers were purchased from eBioscience: CD3ε (clone 145-2C11), CD4 (clone RM4-5), CD11b (clone M1/70), F4/80 (clone BM8), IFNγ (clone XMG1.2), and MHC II (clone M5/114.15.2); from BD Bioscience: SiglecF (clone ES0-2440); and from Biolegend: CD8α (clone 53-6.7), CD11c (clone N418), CD19 (clone 6D5), CD45 (clone 30-F11), CX3CR1 (clone SA011F11), TCRγδ (clone GL3), Ly6C (clone HK1.4), Ly6G (clone 1A8), NKp46 (clone 29A1.4), and NK1.1 (clone PK136). Cells were analyzed on a FACS Fortessa (BD Bioscience). For NK cell and T-cell intracellular cytokine staining, cells from lung or spleen were stimulated with phorbol 12-myristate 13-acetate (PMA; 50 ng/mL; Sigma), ionomycin (1 μg/mL; Sigma), brefeldin-A (10 μg/mL; Sigma), and 2 μmol/L monensin (eBioscience) for 4 hours at 37°C. Cells were treated with Zombie Violet (BioLegend) or LIVE/DEAD Fixable Near-IR stain to exclude dead cells and then stained for surface markers, fixed, and permeabilized using the Foxp3/Transcription Factor Staining Buffer set (eBioscience) following the manufacturer's instructions, and then incubated for 30 minutes at room temperature with the following from eBioscience: anti-IFNγ (clone XMG1.2) and anti-perforin (clone eBioMAK-D); and from Biolegend: anti-granzyme B (clone GB11) and anti-TNFα (clone MP6-XT22). Data were acquired on a FACS Fortessa (BD Bioscience) and analyzed using FACS Diva or FlowJo software (TreeStar).

Ex vivo intracellular TNFα and IL1β staining for myeloid populations was performed on isolated cells 6 hours following an i.v. injection of brefeldin A (10 mg/g of body weight). Lung digestion was performed in the presence of brefeldin A (10 μg/mL). Cells were then stained for surface markers, fixed, permeabilized as described above, and then stained with anti-mouse anti-IL1β (clone NJTEN3; eBioscience), anti-NOS2 (clone CXNFT; eBioscience), and anti-mouse anti-TNFα (clone MP6-XT22; Biolegend).

ELISA

Lungs were perfused with PBS and homogenized using a tissue homogenizer in 0.5 mL PBS containing 0.05% Tween-20 and complete, EDTA-free Protease Inhibitor Cocktail (Roche). The

Published OnlineFirst August 15, 2017; DOI: 10.1158/2326-6066.CIR-17-0082

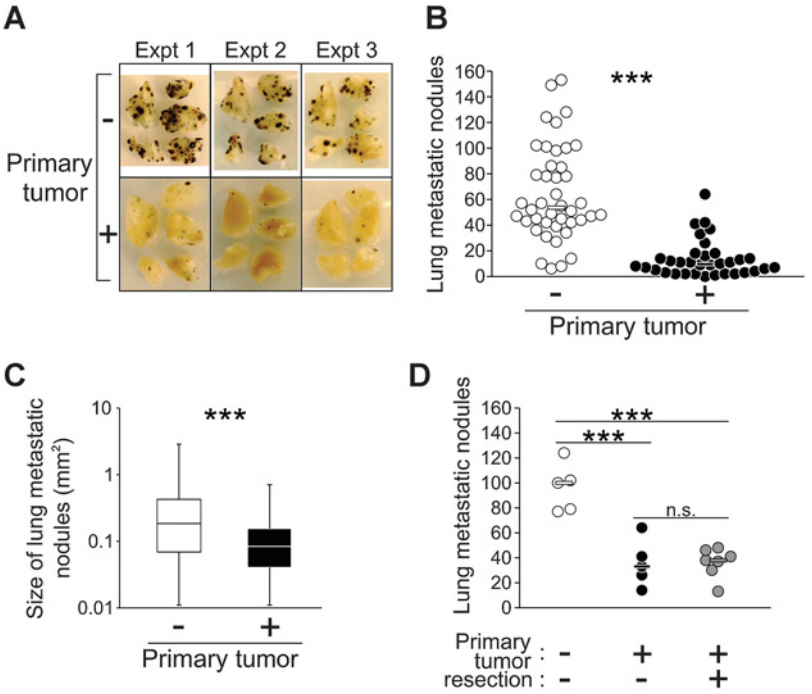

Figure 1.

Primary B16F10 tumor inhibits experimental metastasis formation in the lung. **A,** Representative pictures of pulmonary metastatic nodules produced on day 14 after intravenous injection of 5×10^4 B16F10 cells. Data derive from three independent experiments (Expt). **B,** C57BL/6 mice were injected with PBS ($n = 42$) or B16F10 melanoma cells ($n = 34$) subcutaneously in the flank for establishment of primary tumor. On day 7 after tumor establishment, mice were injected with B16F10 cells (1×10^5) intravenously via tail vein. Lungs were resected on day 14 after the i.v. injection and metastatic nodules were quantified. **C,** The size of each superficial nodule was measured by ImageJ software. The five lobes of the lungs from 5 mice without and 10 mice with primary tumor from 3 independent experiments were analyzed (numbers of colonies; $n = 514, 127$, respectively). **D,** Tumor resection was performed (gray circles) on the same day as metastasis induction in one of three experimental groups ($n = 5$–7 for each group). Each circle represents one animal. ***, $P < 0.001$ (B and C: unpaired two-tailed *t* test; D: one-way ANOVA followed by Bonferroni multiple comparison test).

homogenates were centrifuged at 6,000 × *g* for 10 minutes at 4°C. The supernatant was collected and incubated with recombinant mouse IL15Rα-Fc (500 pg/mL; R&D Systems) for 30 minutes. The concentration of IL15 in the supernatant was evaluated using the mouse IL15R/IL15 Complex ELISA Ready-SET-Go (eBioscience) according to the manufacturer's recommendations.

Statistical analysis

Statistical testing was performed using GraphPad Prism (GraphPad Software Inc.). All data were analyzed by a two-tailed unpaired t test with 95% confidence intervals or one-way ANOVA followed by Bonferroni multiple comparison test, with data representing the mean; *, $P < 0.05$; **, $P < 0.01$; ***, $P < 0.001$ were considered to be statistically significant.

Results

Primary tumors suppress experimental metastasis

We set up a two-step experimental model to determine the effect of primary tumors on the establishment of lung metastasis. Mice in the test group received 5×10^4 B16F10 melanoma cells subcutaneously (s.c.) in the flank. One week later, when B16F10 cells had established visible s.c. tumor lesions (diameter <2 mm), 1×10^5 B16F10 cells were injected i.v. to mimic metastasis formation. Control mice received i.v. B16F10 cells only. Blood-disseminated B16F10 cells preferentially localized to the lungs and formed black colonies easily distinguishable from normal tissue (Fig. 1A). We found 5-fold more metastatic nodules in the lungs of primary tumor-free mice compared with primary tumor-bearing mice (Fig. 1A and B). Colonies established in primary tumor-bearing mice were 2-fold smaller than those in primary tumor-free mice (Fig. 1C). The protective effect of s.c. primary tumor establishment was also observed on abdominal lesions derived from the i.p. injection of secondary B16F0 cells (Supplementary Fig. S1A–S1B). Our results also showed that B16 primary tumors from both F10 and F0 sublines inhibited lung metastasis (i.v.) of E0771 breast cancer cells, which was also suppressed by primary (s.c.) E0771 cell inoculation (Supplementary Fig. S1C). These data collectively suggest a broad activity spectrum for the underlying protective mechanism.

We next aimed to assess whether competition for essential nutrients (the athrepsia hypothesis; refs. 13, 14), or increase in circulating angiogenesis inhibitors, such as angiostatin and endostatin (15–17), accounted for the inhibition of lung metastases by the subcutaneous primary tumor. To do so, we surgically removed primary tumors before, but on the same day of, i.v. B16F10 metastasis induction. We confirmed that no relapse occurred during the time frame of the metastasis formation and analysis. Even when resected, the previous presence of primary tumors (on day 7 or 14) was sufficient to inhibit lung metastases when compared with sham-operated mice (Fig. 1D; Supplementary Fig. S1D). These results suggest that competition for nutrients and/ or survival factors do not account for metastasis inhibition by the primary tumor. Instead, we hypothesized that the host immune response to primary tumors would protect from metastases.

NK cells inhibit experimental metastasis formation in primary tumor-bearing mice

Several lines of evidence point toward NK cells in regulating metastasis formation in B16F10 experimental lung metastasis model (18, 19). Thus, we next assessed the number of NK cells and their activation status within the lung after metastasis induction in primary tumor-bearing versus primary tumor-free mice (gating strategies in Supplementary Fig. S2A–S2B). NK cell numbers and activation peaked on day 2 after metastasis challenge in primary tumor-bearing mice compared with controls (Fig. 2A). Lung NK cells in primary tumor-bearing mice displayed higher expression of CD11b (maturation marker of NK cells), granzyme B, perforin, and IFNγ (Fig. 2A; Supplementary Fig. S2C). This was

Published OnlineFirst August 15, 2017; DOI: 10.1158/2326-6066.CIR-17-0082

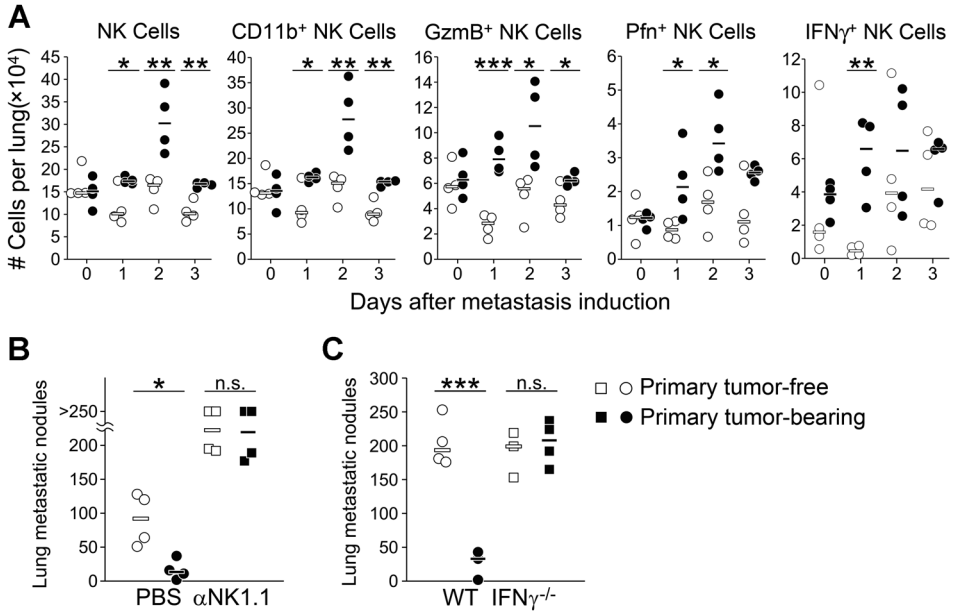

Figure 2.
Experimental metastasis inhibition by primary tumors is mediated by NK cells and IFNγ. **A,** Total cell numbers of NK cells and NK cell activation status in the lungs on days 0, 1, 2, and 3 after metastasis induction in primary tumor-free (open symbols) or tumor-bearing (closed symbols) mice ($n = 4$ for each group). Data are representative of two independent experiments. **B,** Number of B16F10 lung metastatic nodules in primary tumor-free or primary tumor-bearing mice (as in Fig. 1B) upon NK cell depletion using anti-NK1.1 mAb ($n = 4$ for each group. **C,** B16F10 lung metastatic nodules in IFNγ$^{-/-}$ mice in the presence or absence of primary tumor ($n = 3$–4 for each group). Each symbol represents one animal. *, $P < 0.05$; **, $P < 0.01$; ***, $P < 0.001$ (unpaired two-tailed t test).

specific to the lung as no alterations were observed in the spleen upon metastatic challenge (Supplementary Fig. S2D). To formally test whether NK cells contributed to metastasis inhibition by the primary tumor, we injected anti-NK1.1 mAb, which resulted in very efficient depletion of NK cells (Supplementary Fig. S2E). In the absence of NK cells, the protective effect of primary tumors on metastasis formation was completely abolished (Fig. 2B), and a significant increase in the number of metastatic foci was observed in primary tumor-free mice upon NK cell depletion (Fig. 2B). This is consistent with previous reports on NK cell–mediated elimination of lung B16F10 metastases (9, 18). Thus, our data support the key role of NK cells in controlling metastasis formation and add to it by demonstrating that primary tumors are responsible for further activation of the protective NK cell response.

IFNγ-producing NK cells have been reported to play an early protection against metastasis (20, 21). Therefore, given that we observed a rapid increased in IFNγ-producing NK cells upon metastasis challenge (Fig. 2A), we went on to determine if IFNγ played a role in inhibiting lung metastasis. We observed a clear loss of the protective effect of the primary tumor in IFNγ$^{-/-}$ mice compared with WT controls (Fig. 2C), thus implicating IFNγ production as a key molecular mechanism underlying metastasis suppression in primary tumor-bearing mice. Although the phenotype in IFNγ$^{-/-}$ mice cannot be directly ascribed to NK cells, the contribution of IFNγ-producing NK cells, compared with IFNγ-producing T cells, increased in primary tumor-bearing mice (Supplementary Fig. S3A–S3D).

M1-like myeloid cells accumulate in the lungs of primary tumor-bearing mice

We next set out to dissect the link between the primary (s.c.) tumor and the accumulation and activation of NK cells in the lung. It is well known that the number and functions of NK cells depend on the cytokine environment and on cell-to-cell interactions with myeloid cells such as monocytes, macrophages, and neutrophils (22–27). We, therefore, monitored myeloid populations in the lung in response to metastasis induction (gating strategies in Supplementary Fig. S4A). Patrolling (CX3CR1^{+} LY6C^{-}) and classical (CX3CR1^{-} LY6C^{+}) monocytes, macrophages, and alveolar macrophages all accumulated from day 1 after metastasis challenge in primary tumor-bearing mice (Fig. 3A). This accumulation was specific to the lung as neither patrolling monocytes nor macrophages were altered in the spleen (Supplementary Fig. S4B). In contrast, in the bone marrow of primary tumor-bearing mice, only patrolling monocytes increased after metastasis induction (Supplementary Fig. S4C), and they expressed significantly more CD115 [also known as macrophage colony-stimulating factor (M-CSF) receptor or CSF1 receptor] than classical monocytes or macrophages (Supplementary Fig. S4D; refs. 28–30). The kinetics of these myeloid populations, including monocyte subsets and macrophages, mirrored that of NK cells, suggesting they might cooperate in preventing metastasis formation in primary tumor-bearing mice.

We also analyzed the activation and polarization status of patrolling and classical monocytes and macrophages in the lung (Supplementary Fig. S4E). In mice, classically activated M1 macrophages, which are associated with antitumor functions, are characterized by increased microbicidal activity, including the expression of NO synthase 2 (NOS2) and high antigen-presenting activity linked to increased MHC class II expression (31). Two days after metastasis induction in primary tumor-bearing mice, the expression of MHC class II molecules and NOS2 was increased in both cell types (Fig. 3B), and macrophages expressed more TNFα and less IL1β in the presence of primary tumor. TNFα is a key cytokine to block the protumor M2 polarization (32). In contrast, expression of MHC class II, NOS2, and IL1β did not change, whereas TNFα was even lower in classical monocytes of primary tumor-bearing mice (Fig. 3B). Collectively, these data suggest an M1-like (antitumor) polarization of patrolling monocytes and macrophages at the metastatic site of primary tumor-bearing mice. Also, given that patrolling monocytes and macrophages in the lung shared similar polarization status, it is possible that the former give rise to the latter, as previously proposed (33).

Published OnlineFirst August 15, 2017; DOI: 10.1158/2326-6066.CIR-17-0082

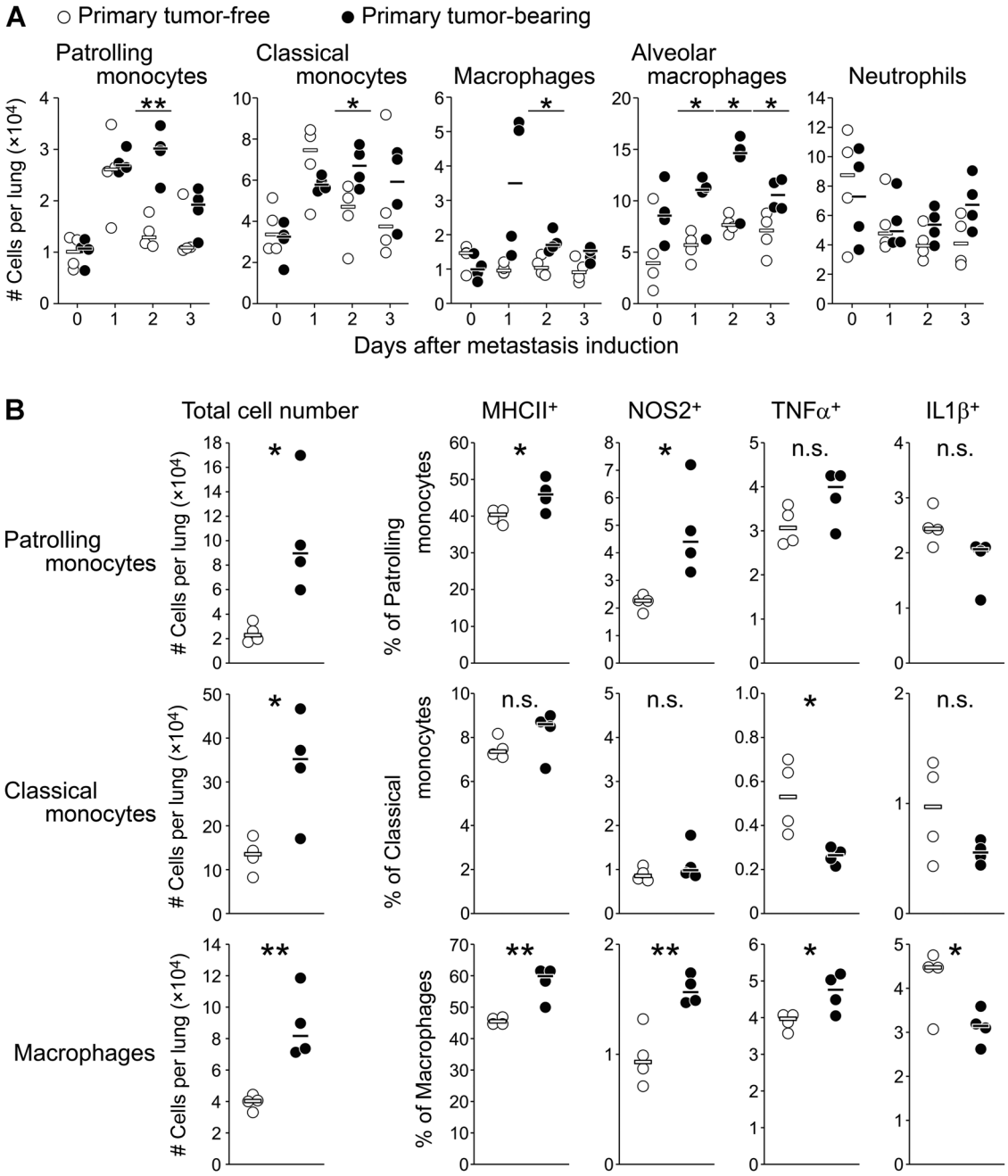

Figure 3.

Primary tumors induce a myeloid response dominated by M1-like monocytes and macrophages. **A,** Total cell numbers of myeloid populations in the lungs on days 0, 1, 2, and 3 after metastasis induction in mice without (open circles) or with (closed circles) primary tumor. Data are representative of two independent experiments ($n = 4$ for each group). **B,** Activation and polarization status of monocytes (patrolling and classical) and macrophages (analyzed as in Supplemental Fig. 2) in the lungs of primary tumor-free versus primary tumor-bearing mice on day 2 after metastasis induction ($n = 4$ for each group). Each circle represents one animal. *, $P < 0.05$; **, $P < 0.01$ (unpaired two-tailed t test).

Patrolling monocytes activate NK cells via IL15 to control metastasis formation

To assess the contribution of these myeloid cells, we used a depleting antibody against CD115, which is expressed on monocytes and macrophages (34) but significantly higher on patrolling monocytes (Supplementary Fig. S4D). We found that anti-CD115 mAb injection in primary tumor-free or primary tumor-bearing mice was efficient at depleting only patrolling monocytes from the bone marrow, blood, and lung (Supplementary Figs. S4C and S5A–S5B) and resulted in an abrogation of the NK cell response (numbers and functional properties) in the lung of primary tumor-bearing mice (Fig. 4A; Supplementary Fig. S3D),

Published OnlineFirst August 15, 2017; DOI: 10.1158/2326-6066.CIR-17-0082

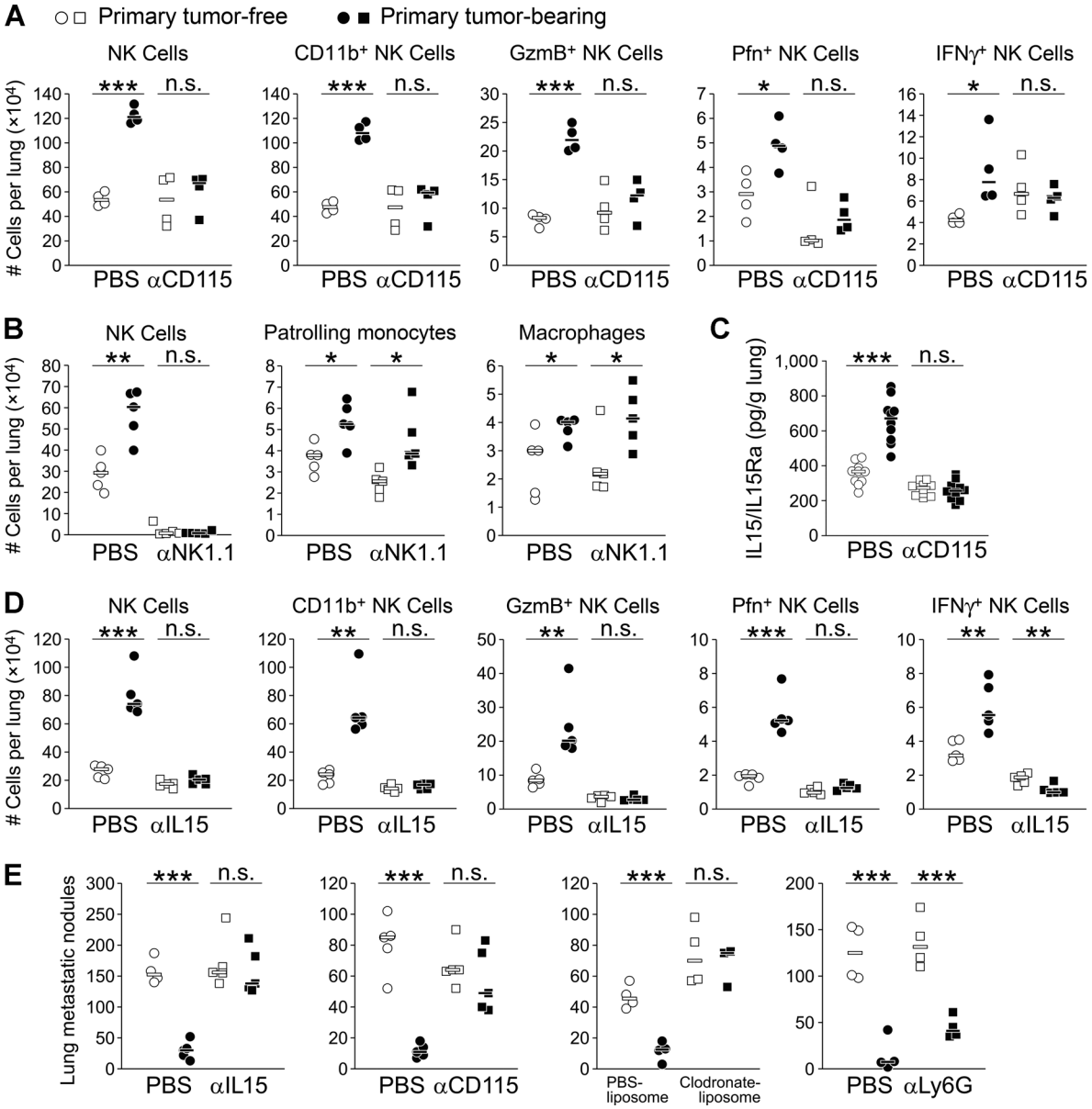

Figure 4.

Patrolling monocytes activate NK cells via IL15 to prevent lung metastases in primary tumor-bearing mice. **A,** The effect of depleting patrolling monocytes on total NK cell numbers and activation status on day 2 after metastasis induction in the lungs of mice with (closed symbols) or without (open symbols) primary tumors ($n = 4$ for each group). **B,** Total NK cell, patrolling monocyte, and macrophage numbers on day 2 after metastasis induction in the lungs of mice with or without primary tumor (circles) and upon NK cell depletion using anti-NK1.1 mAb (squares; $n = 5$ for each group). **C,** ELISA quantification of total IL15 in the lungs on day 2 after metastasis induction of primary tumor-free versus primary tumor-bearing mice (circles) and upon anti-CD115 mAb administration (squares; $n = 10$ for each group). **D,** The effect of IL15 neutralization on total NK cell numbers and activation status on day 2 after metastasis induction in the lungs of mice with (closed symbols) or without (open symbols) primary tumors ($n = 5$ for each group). **E,** Number of B16F10 lung metastatic nodules in primary tumor-free or primary tumor-bearing mice (as in Fig. 1B) and upon IL15 neutralization or depletion of monocytes and macrophages or neutrophils ($n = 3$-5 for each group). Each symbol represents one animal. *, $P < 0.05$; **, $P < 0.01$; ***, $P < 0.001$ (unpaired two-tailed t test).

suggesting that patrolling monocytes are upstream of NK cells in preventing metastasis formation. Conversely, NK cell depletion did not affect the accumulation of patrolling monocytes or macrophages in the lung (Fig. 4B).

Trying to further dissect the link between patrolling monocytes and NK cells, we looked into IL15, because it is the dominant cytokine for NK cell homeostasis (35) and can be abundantly produced by monocytes and macrophages (33, 36). We measured the amount of IL15/soluble IL15Rα in the lungs of primary tumor-bearing mice in response to metastasis induction. Our results showed 2-fold higher amounts of IL15 in lungs of primary tumor-bearing mice compared with primary tumor-free mice

Published OnlineFirst August 15, 2017; DOI: 10.1158/2326-6066.CIR-17-0082

(Fig. 4C). Depletion of patrolling monocytes using antibody to CD115 resulted in an abrogation of the increase of IL15 production in the lungs of primary tumor-bearing mice after metastasis challenge (Fig. 4C). This shows that the IL15 response to primary tumors is mediated by patrolling monocytes. Next, to explore the role of the IL15 response in downstream NK cell activation, we blocked IL15 using an antagonizing antibody. Neutralization of IL15 led to abrogation of lung NK cell accumulation and effector functions upon metastasis formation in primary tumor-bearing mice (Fig. 4D). On the other hand, IL15 neutralization did not affect the increase of patrolling monocytes and macrophages in the lungs of primary tumor-bearing mice (Supplementary Fig. S5C), further establishing IL15 downstream of patrolling monocytes in the response to primary tumors.

Finally, to assess the contribution of IL15 and monocytes and macrophages in the prevention of metastasis to the lungs of primary tumor-bearing mice, we used anti-IL15 mAb, anti-CD115 mAb, and clodronate-loaded liposomes. Clodronate liposomes are taken up and eliminate phagocytic cells such as monocytes and macrophages (37). Treatment with clodronate liposomes effectively depleted circulating macrophages and patrolling monocytes but not classical monocytes (Supplementary Fig. S5A). Both IL15 neutralization and the depletion of patrolling monocytes and macrophages completely abolished the inhibitory effect of the primary tumors on metastasis formation (Fig. 4E). In contrast, neutrophil depletion using anti-Ly6G mAb did not affect metastasis inhibition (Fig. 4E). Although clodronate liposomes depleted patrolling monocytes, macrophages, and alveolar macrophages in the lungs, anti-CD115 mAb mainly depleted patrolling monocytes (Supplementary Fig. S5B). These data collectively suggest that patrolling monocytes are the key myeloid population to convey the inhibition of metastasis in the presence of primary tumors, and that IL15 is the molecular link to NK cells and their antimetastatic effector functions.

Discussion

Our studies investigated how the immune response to the primary tumor may affect metastasis formation during cancer progression. We demonstrated that the primary tumor sets up an innate immune cell network responsible for metastasis immunosurveillance. Patrolling monocytes respond to the primary tumor by producing IL15, which activates the antimetastatic activities of NK cells, particularly IFNγ production that is essential for protection. NK cell depletion, but not monocyte elimination, led to a significant increase in metastatic colonies established in primary tumor-free mice. Thus, NK cells seem to play two types of antimetastatic roles in primary tumor-free versus primary tumor-bearing mice. In support of this postulate, our data showed that IFNγ was required for metastasis inhibition in primary tumor-bearing mice, whereas previous reports have shown that IFNγ was dispensable for the rapid NK cell–mediated elimination of lung B16F10 metastases in the absence of primary tumors (18).

A key finding of our study is the role played by primary tumors in setting up the innate immune network of patrolling monocytes and NK cells. This was only possible due to our two-step experimental model that allowed us to analyze the immune response to primary tumors first and then assess its impact on metastases formation. Although our conclusions based on this experimental model cannot be directly extrapolated to spontaneous metastasis formation, they are strengthened by the consistency of three distinct settings in which B16 primary tumors inhibited the development of secondary B16 tumors in the lung and in the peritoneum (derived from i.v. versus i.p. secondary injections) and suppressed the experimental metastases of (i.v.) E0771 breast cancer cells to the lung. Our data provide evidence that innate immune cross-talk is a potent component of metastasis immunosurveillance.

A study by Kirstein and colleagues showed reduced experimental metastases in mice bearing a primary B16F10 tumor (compared with controls without a primary tumor), but this was attributed to a reduction of circulating platelets and reduced formation of metastatic tumor cell–associated thrombi (38). Mice in that study developed splenomegaly (correlated with primary tumor size), which we did not observe in our experiments. Concomitant antimetastatic effects of primary tumors may consist of nonimmunological and/ or immune-mediated mechanisms (39). Our results support the latter, with the dissected cellular and molecular mechanisms building on the study by Hanna and colleagues that identified an antimetastatic role for nonclassical patrolling monocytes through the recruitment of NK cells (9). Our work adds to this by showing that primary tumors trigger an IL15 response from patrolling monocytes which activate NK cells to secrete IFNγ that inhibit metastasis. Although we cannot discount NK cell recruitment via the chemokines CCL3, CCL4, and CCL5 as previously suggested (9), we propose here a dominating role for IL15 in the cross-talk between patrolling monocytes (whose activation mechanisms are still to be dissected) and NK cells. Monocyte-derived IL15 has long been known to be critical for IFNγ production by NK cells (36), and IFNγ is a crucial cytokine in cancer immunoediting (40, 41). Our data suggest that NK cells increase rapidly in primary tumor-bearing mice due to the help of patrolling monocytes, which results in the elimination of metastasizing B16F10 cells at the earlier stages of attachment to the lung endothelium and establishment of the initial colonies.

At a time when the manipulation of adaptive immunity is already producing therapeutic benefit in cancer immunotherapy, this study focuses on innate immunity and consolidates the patrolling monocyte/ NK cell axis as the key determinant of metastasis immunosurveillance. As such, our data show that the manipulation of this innate cellular network, via its key molecular mediator, IL15, has potential for future cancer immunotherapeutic approaches.

IL15 is a key determinant of NK cell homeostasis, activation, and effector functions (35, 42). Although NK cell–based immunotherapy has thus far met with limited clinical success (43), Huntington and colleagues identified a critical negative regulator of IL15 signaling in NK cells (44) that may underlie the difficulty in harnessing the tumor-killing abilities of NK cells. Cytokine-inducible SH2-containing protein (CIS) interacted with the tyrosine kinase JAK1, inhibiting its enzymatic activity and targeting it for proteasomal degradation, thus blocking IL15 signaling. Genetic ablation of CIS rendered NK cells hyperresponsive to IL15, as evidenced by enhanced proliferation, survival, IFNγ production, and cytotoxicity toward tumors and resulted in resistance to melanoma, prostate, and breast cancer metastasis *in vivo* (44). Thus, CIS-mediated regulation of IL15 signaling seems to be a potent intracellular checkpoint in NK cell–mediated tumor immunity. Given the impact of T-cell checkpoint inhibitors on cancer treatment, overcoming NK cell inhibition (e.g., via CIS blockade) may hold the key to translate the enormous antitumor

Published OnlineFirst August 15, 2017; DOI: 10.1158/2326-6066.CIR-17-0082

(and antimetastasis) potential of NK cells into clinical benefit for cancer patients.

Disclosure of Potential Conflicts of Interest

No potential conflicts of interest were disclosed.

Authors' Contributions

Conception and design: H. Kubo, B. Silva-Santos
Development of methodology: H. Kubo, N. Gonçalves-Sousa, K. Serre
Acquisition of data (provided animals, acquired and managed patients, provided facilities, etc.): H. Kubo, N. Gonçalves-Sousa
Analysis and interpretation of data (e.g., statistical analysis, biostatistics, computational analysis): H. Kubo, S. Mensurado, N. Gonçalves-Sousa, K. Serre
Writing, review, and/or revision of the manuscript: H. Kubo, K. Serre, B. Silva-Santos
Administrative, technical, or material support (i.e., reporting or organizing data, constructing databases): S. Mensurado
Study supervision: B. Silva-Santos

Acknowledgments

We thank Francisco Caiado, Ana Água-Doce, Pedro Papotto (iMM Lisboa), and Jai Rautela (Walter & Eliza Institute, Melbourne) for help and advice; and the flow cytometry and animal facilities of iMM Lisboa for technical support.

Grant Support

This work was funded by the European Research Council (CoG_646701 to B. Silva-Santos). S. Mensurado (PD/BD/114099/2015) and K. Serre (IF/00004/2014) acknowledge their individual funding from Fundação para a Ciência e Tecnologia.

The costs of publication of this article were defrayed in part by the payment of page charges. This article must therefore be hereby marked *advertisement* in accordance with 18 U.S.C. Section 1734 solely to indicate this fact.

Received February 8, 2017; revised May 31, 2017; accepted July 27, 2017; published OnlineFirst August 15, 2017.

References

1. Leone P, Shin EC, Perosa F, Vacca A, Dammacco F, Racanelli V. MHC class I antigen processing and presenting machinery: organization, function, and defects in tumor cells. J Natl Cancer Inst 2013;105:1172–87.
2. Dosani T, Carlsten M, Maric I, Landgren O. The cellular immune system in myelomagenesis: NK cells and T cells in the development of MM and their uses in immunotherapies. Blood Cancer J 2015;5:e306.
3. DeNardo DG, Andreu P, Coussens LM. Interactions between lymphocytes and myeloid cells regulate pro-versus anti-tumor immunity. Cancer Metastasis Rev 2010;29:309–16.
4. Lança T, Silva-Santos B. The split nature of tumor-infiltrating leukocytes: implications for cancer surveillance and immunotherapy. Oncoimmunology 2012;1:717–25.
5. Biswas SK, Mantovani A. Macrophage plasticity and interaction with lymphocyte subsets : cancer as a paradigm. Nat Immunol 2010;11:889–96.
6. Fridlender ZG, Sun J, Kim S, Kapoor V, Cheng G, Ling L, et al. Polarization of tumor-associated neutrophil phenotype by TGF-beta: "N1" versus "N2" TAN. Cancer Cell 2009;16:183–94.
7. Cassetta L, Pollard JW. Cancer immunosurveillance: role of patrolling monocytes. Cell Res 2015;26:3–4.
8. Qian B, Li J, Zhang H, Kitamura T, Zhang J, Liam R, et al. CCL2 recruits inflammtatory monocytes to facilitate breast tumour metastasis. Nature 2012;475:222–5.
9. Hanna RN, Cekic C, Sag D, Tacke R, Thomas GD, Nowyhed H, et al. Patrolling monocytes control tumor metastasis to the lung. Science 2015;350:985–90.
10. Chambers AF, Groom AC, MacDonald IC. Dissemination and growth of cancer cells in metastatic sites. Nat Rev Cancer 2002;2:563–72.
11. Hüsemann Y, Geigl JB, Schubert F, Musiani P, Meyer M, Burghart E, et al. Systemic spread is an early step in breast cancer. Cancer Cell 2008;13:58–68.
12. Klein CA. Parallel progression of tumour and metastases. Nat Rev Cancer 2010;10:156.
13. Bashford E, Murray J, Cramer W. The natural and induced resistance of mice to the growth of cancer. Proc R Soc London Ser B, Contain Pap a Biol Character 1907;79:164–87.
14. Tyzzer EE. Factors in the production and growth of tumor metastases. J Med Res 1913;28:309–33.
15. O'Reilly MS, Holmgren L, Shing Y, Chen C, Rosenthal RA, Moses M, et al. Angiostatin: A novel angiogenesis inhibitor that mediates the suppression of metastases by a lewis lung carcinoma. Cell 1994;79:315–28.
16. Holmgren L, O'Reilly MS, Folkman J. Dormancy of micrometastases: balanced proliferation and apoptosis in the presence of angiogenesis suppression. Nat Med 1995;1:149–53.
17. Folkman J. Angiogenesis in cancer, vascular, rheumatoid and other disease. Nat Med 1995;1:27–31.
18. Grundy MA, Zhang T, Sentman CL. NK cells rapidly remove B16F10 tumor cells in a perforin and interferon-gamma independent manner in vivo. Cancer Immunol Immunother 2007;56:1153–61.
19. Eckelhart E, Warsch W, Zebedin E, Simma O, Stoiber D, Kolbe T, et al. A novel Ncr1-Cre mouse reveals the essential role of STAT5 for NK-cell survival and development. Blood 2015;117:1565–74.
20. Street SE, Cretney E, Smyth MJ. Perforin and interferon-gamma activities independently control tumor initiation, growth, and metastasis. Blood 2001;97:192–7.
21. Kasamatsu J, Azuma M, Oshiumi H, Morioka Y, Okabe M, Ebihara T, et al. INAM Plays a critical Role in IFN- production by NK cells interacting with polyinosinic-polycytidylic acid-stimulated accessory cells. J Immunol 2014;193:5199–207.
22. Jaeger BN, Donadieu J, Cognet C, Bernat C, Ordonez-Rueda D, Barlogis V, et al. Neutrophil depletion impairs natural killer cell maturation, function, and homeostasis. J Exp Med 2012;209:565–80.
23. Marceau K, Ruttle PL, Shirtcliff EA, Essex MJ, Susman EJ, Studies A, et al. HHS Public Access2015;57:742–68.
24. Michel T, Hentges F, Zimmer J. Consequences of the crosstalk between monocytes/macrophages and natural killer cells. Front Immunol 2012;3:1–7.
25. Amano K, Hirayama M, Azuma E, Iwamoto S, Keida Y, Komada Y. Neutrophils induced licensing of natural killer cells. Mediators Inflamm 2015;2015.
26. Ueda R, Narumi K, Hashimoto H, Miyakawa R, Okusaka T, Aoki K. Interaction of natural killer cells with neutrophils exerts a significant antitumor immunity in hematopoietic stem cell transplantation recipients. Cancer Med 2016;5:49–60.
27. Vivier E. Functions of natural killer cells. Nat Immunol 2008;9:503–10.
28. Louis C, Cook AD, Lacey D, Fleetwood AJ, Vlahos R, Anderson GP, et al. Specific contributions of CSF-1 and GM-CSF to the dynamics of the mononuclear phagocyte system. J Immunol 2015;195:134–44.
29. Greter M, Helft J, Chow A, Hashimoto D, Mortha A, Agudo-Cantero J, et al. GM-CSF controls nonlymphoid tissue dendritic cell homeostasis but is dispensable for the differentiation of inflammatory dendritic cells. Immunity 2012;36:1031–46.
30. Fend L, Accart N, Kintz J, Cochin S, Reymann C, Le Pogam F, et al. Therapeutic effects of Anti-CD115 monoclonal antibody in mouse cancer models through dual inhibition of tumor-associated macrophages and osteoclasts. PLoS One 2013;8.
31. Gordon S, Taylor PR. Monocyte and macrophage heterogeneity. Nat Rev Immunol 2005;5:953–64.
32. Kratochvill F, Neale G, Haverkamp JM, Van de Velde LA, Smith AM, Kawauchi D, et al. TNF counterbalances the emergence of M2 tumor macrophages. Cell Rep 2015;12:1902–14.
33. Doherty TM, Seder RA, Sher A. Induction and regulation of IL-15 expression in murine macrophages. J Immunol 1996;156:735–41.
34. Stanley ER, Chitu V. CSF-1 receptor signaling in myeloid cells2016;1–21.
35. Ranson T, Vosshenrich CAJ, Corcuff E, Richard O, Müller W, Di Santo JP. IL-15 is an essential mediator of peripheral NK-cell homeostasis. Blood 2003;101:4887–93.

Published OnlineFirst August 15, 2017; DOI: 10.1158/2326-6066.CIR-17-0082

36. Carson WE, Ross ME, Baiocchi RA, Marien MJ, Boiani N, Grabstein K, et al. Endogenous production of interleukin 15 by activated human monocytes is critical for optimal production of interferon-gamma by natural killer cells in vitro. J Clin Invest 1995;96:2578–82.
37. Gibbons MA, MacKinnon AC, Ramachandran P, Dhaliwal K, Duffin R, Phythian-Adams AT, et al. Ly6Chi monocytes direct alternatively activated profibrotic macrophage regulation of lung fibrosis. Am J Respir Crit Care Med 2011;184:569–81.
38. Kirstein JM, Hague MN, Mcgowan PM, Tuck AB. Primary melanoma tumor inhibits metastasis through alterations in systemic hemostasis. J Mol Med 2016;65:787–800.e5.
39. Nomi S, Naito K, Kahan BD, Pellis NR. Effects of concomitant and sinecomitant immunity on postsurgical metastasis 1986;6111–5.
40. Dunn GP, Bruce AT, Diamond M, White JM, Sheehan KCF, Schreiber RD. Interferon-γ and Cancer2005;231–45.
41. O'Sullivan T, Saddawi-Konefka R, Vermi W, Koebel CM, Arthur C, White JM, et al. Cancer immunoediting by the innate immune system in the absence of adaptive immunity. J Exp Med 2012;209:1869–82.
42. Rautela J, Huntington ND. IL-15 signaling in NK cell cancer immunotherapy. Curr Opin Immunol 2017;44:1–6.
43. Baggio L, Laureano AM, Silla LM, Lee DA. Natural killer cell adoptive immunotherapy: coming of age. Clin Immunol 2016;177:3–11.
44. Delconte RB, Kolesnik TB, Dagley LF, Rautela J, Shi W, Putz EM, et al. CIS is a potent checkpoint in NK cell-mediated tumor immunity. Nat Immunol 2016;17:816–24.

Published OnlineFirst August 15, 2017; DOI: 10.1158/2326-6066.CIR-17-0082

Cancer Immunology Research

Primary Tumors Limit Metastasis Formation through Induction of IL15-Mediated Cross-Talk between Patrolling Monocytes and NK Cells

Hiroshi Kubo, Sofia Mensurado, Natacha Gonçalves-Sousa, et al.

Cancer Immunol Res Published OnlineFirst August 15, 2017.